SYNTHETIC APERTURE RADAR IMAGING USING A UNIQUE APPROACH TO FREQUENCY-MODULATED CONTINUOUS-WAVE RADAR DESIGN

Gregory L. Charvat, MSEE,
Leo C. Kempel, Ph.D.
Department of Electrical and Computer Engineering
Michigan State University
2120 Engineering Building
East Lansing, MI 48825

ABSTRACT

Synthetic Aperture Radar (SAR) imaging is an expensive endeavor. It can be difficult for universities, small business, or individuals to experiment with SAR imaging and algorithm development on a low budget. For this reason, a uniquely inexpensive solution to Frequency-Modulated Continuous-Wave (FMCW) radar was developed and then utilized as an ultra low cost SAR imaging system. This unique approach to FMCW radar uses a pair of low cost Gunn oscillator based microwave transceiver modules known as 'Gunnplexers'. These transceiver modules have stability and noise problems causing them to be unsuitable for use in precise FMCW radar applications when just one module is used. In order to overcome this problem, a unique radar solution was developed which uses a combination of two transceiver modules to create a precise and inexpensive FMCW radar system capable of producing SAR imagery on a budget.

Keywords: FMCW, Gunn Oscillator, Low Cost SAR, Linear SAR, Radar Imaging, Small Aperture SAR

1. Introduction

The objective of this article is to prove that synthetic aperture radar (SAR) imaging on an extremely low budget is possible. This research was conducted by the Michigan State University Electromagnetics Research Group in an effort to expand our research opportunities at a minimum financial risk. A unique approach to frequency-modulated continuous-wave (FMCW) radar design was developed and utilized as an ultra low cost SAR imaging system. This system was then used successfully to develop four different SAR imaging algorithms which have been used in a number of subsequent research projects.

The unique approach to FMCW was previously introduced in [1], [2], and [3]. Section 2 is an explanation of the MA87127-1 Gunn oscillator based transceiver module known as a 'Gunnplexer.' An explanation of the unique approach to FMCW radar is presented in section 3. Range profile results are presented in section 4. Section 5 will explain the SAR system implementation. Section 6 will present imaging results using a range stacking SAR algorithm. Section 7 will present imaging results using two versions of the polar format algorithm (PFA). Section 8 will present imaging results using the range migration algorithm (RMA). Conclusions and future work will be discussed in section 9.

2. The MA87127-1 Transceiver Module

The unique approach to FMCW radar design depends on the use of two inexpensive microwave transceiver modules. These modules are Gunn diode based, and are more commonly known as 'Gunnplexers.' The particular microwave transceiver module used for this system is the M/A-Com model MA87127-1 X-band microwave transceiver module. In practice almost any X-band varactor tuned 'Gunnplexer' could be used to implement this system.

The MA87127-1 is composed of three major components, a voltage controlled oscillator (VCO), mixer, and circulator (see figure 1). The VCO is fed into port 1 of the circulator. Port 2 of the circulator is connected to the WR-90 waveguide flange input/output port of the transceiver. Port 3 of the circulator is connected to the RF input of the mixer. Some power is coupled off the VCO and fed into the Local Oscillator (LO) port of the mixer. The IF output of the mixer is connected to a small solder terminal on the outer case of the transceiver.

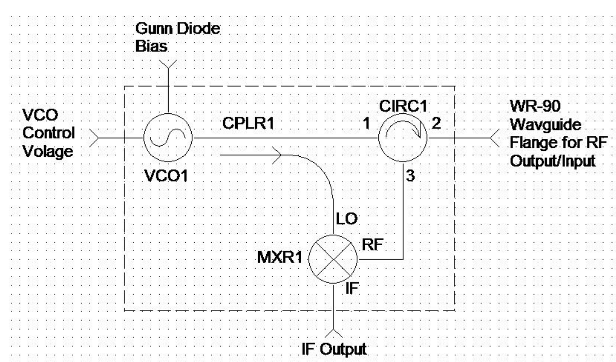

Figure 1: MA87127-1 block diagram.

VCO1 is a varactor controlled Gunn diode oscillator. A varactor diode is placed inside of a cavity Gunn oscillator as shown in figure 2. A bias voltage on the varactor diode between, roughly, 0 and 20 V controls the frequency of the Gunn oscillator. A second bias voltage of approximately 10 V causes the Gunn diode to oscillate at the frequency of the cavity that it is placed in.

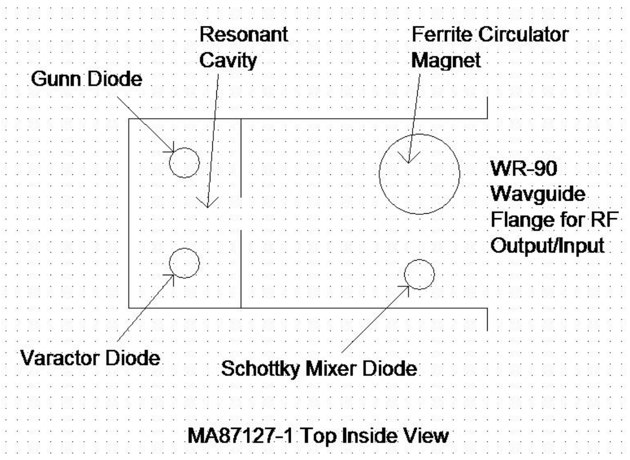

Figure 2: MA87127-1 Physical Layout.

Looking at figure 1, CPLR1 is a symbolic representation of the coupling action that occurs between the Gunn oscillator diode and the Schottky mixer diode placed within close proximity as shown in figure 2.

MXR1 is created by the coupled power from the Gunn diode oscillator. This coupled power causes the Schottky mixer diode to switch on and off. This switching action causes the Schottky mixer diode to operate as a single balanced mixer.

CIRC1 is a ferrite circulator placed inside of the WR90 waveguide that contains MXR1 and that is weakly coupled to the resonant cavity where the Gunn oscillator is located. CIRC1 is basically a large magnet precisely placed inside of the WR90 waveguide section. CIRC1 causes RF power from VCO1 to exit the input/output port, and causes RF power coming into the input/output port to be transferred into MXR1.

When looking at figure 1, it appears as though just one transceiver module alone can be utilized as an FMCW radar system. However, it was found in lab tests that the pass band of the IF port on MXR1 starts to roll off around 1 MHz, causing little to no response at audio frequency, which is were most beats from a short range FMCW radar system will be located. The transceiver module's receiver worked most efficiently at IF frequencies above 30 MHz, where the loss due to the mixer was found to be the least. The lack of an acceptable low frequency to near DC response from MXR1 renders one individual transceiver module useless for most short range FMCW radar applications.

Regardless of its shortcomings, when two MA87127-1 (or similar) transceiver modules are used together, the unique FMCW radar design solution can be obtained.

3. The Unique Approach to FMCW Radar

In order to fully understand the unique approach to FMCW radar, the reader must be well versed in the theoretical operation of FMCW radar systems. A good explanation of FMCW radar can be found in [4]. The unique approach to FMCW radar was implemented using two low cost MA87127-1 Gunn diode based transceiver modules. All schematics and further explanation of this design can be found in [1]. A picture of the system is shown in figure 3. Figure 4 shows a simplified block diagram of the FMCW radar system.

Figure 3: A unique approach to FMCW radar.

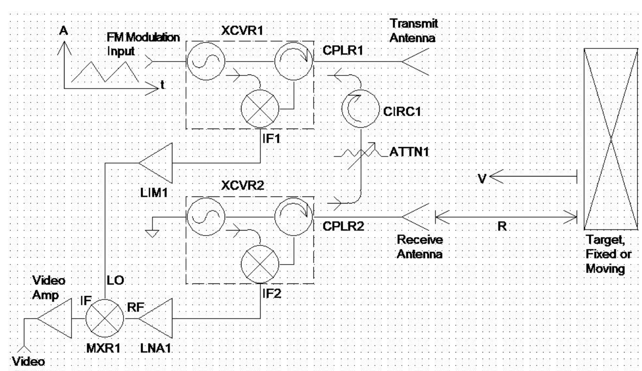

Figure 4: Simplified block diagram of the unique FMCW radar solution.

The following is a mathematical explanation of the unique approach to FMCW radar. The MA87127-1 transceiver module XCVR1 is centered at frequency f_1 and FM modulated with a linear chirp, kf_d, where $k = \frac{volts}{\sec ond}$. The output of XCVR1 is represented by the equation:

$$TX_1(t) = \cos[2\pi f_1 t + 2\pi k f_d] \tag{1}$$

The output of XCVR1 is fed into the transmit antenna. The transmitted signal is radiated out toward the target scene then reflected off of the target. The target is situated at a range R and moving at a velocity v (if it is moving). The range R and velocity v correspond to a time difference and Doppler shift between the original transmit signal and that which was picked up by the receive antenna and fed into the MA87127-1 transceiver module XCVR2. This time difference corresponds to a beat frequency difference f_b as shown in [4]. Thus, the reflected signal from the target is represented by the equation:

$$TX_{1b}(t) = \cos[2\pi f_1 t + 2\pi k f_d + 2\pi f_b t] \tag{2}$$

XCVR2 is set to a fixed frequency of f_2. XCVR2 is radiating a fixed frequency carrier at that frequency which can be represented by the equation:

$$TX_2(t) = \cos[2\pi f_2 t] \tag{3}$$

As explained in section 2, the IF output of each transceiver module is a product of its VCO frequency and any RF power that is coming into the input/output port of the module. Because of this, the IF output of XCVR2 can be calculated:

$$\begin{aligned} IF_2(t) &= TX_{1b}(t) TX_2(t) \\ &= \frac{1}{2}\cos[2\pi f_1 t + 2\pi k f_d t + 2\pi f_b t + 2\pi f_2 t] + \\ &+ \frac{1}{2}\cos[2\pi f_1 t + 2\pi k f_d t + 2\pi f_b t - 2\pi f_2 t] \end{aligned} \tag{4}$$

The higher frequency term can be dropped. This is a practical consideration since the IF output port of the transceiver modules is not capable of producing X-band microwave signals. Thus, the IF output of XCVR2 can be simplified as:

$$IF_2(t) = \frac{1}{2}\cos[2\pi f_1 t + 2\pi k f_d t + 2\pi f_b t - 2\pi f_2 t] \tag{5}$$

Simultaneously, some power from XCVR2 is coupled into XCVR1, taking advantage of a coupling problem that would otherwise limit a typical FMCW radar system. Power from XCVR2 is deliberately coupled out using CPLR2 and output through ATT1, CIRC1, and into CPLR1. The coupled power injected into CPLR1 is fed into XCVR1. The resulting frequency response at the IF port of XCVR1 is calculated using the equation:

$$\begin{aligned} IF_1(t) &= TX_2(t) TX_1(t) \\ &= \frac{1}{2}\cos[2\pi f_2 t + 2\pi f_1 t + 2\pi k f_d t] + \\ &+ \frac{1}{2}\cos[2\pi f_2 t - 2\pi f_1 t - 2\pi k f_d t] \end{aligned} \tag{6}$$

Like XCVR2, the higher frequency term can be dropped. Thus, the IF output of XCVR1 can be simplified as:

$$IF_1(t) = \frac{1}{2}\cos[2\pi f_2 t - 2\pi f_1 t - 2\pi k f_d t] \tag{7}$$

$IF_1(t)$ is fed into the input port of a limiting amplifier, LIM1. The output of LIM1 is used as the LO drive of MXR1. $IF_2(t)$ is fed into the input port of an LNA, which is represented by LNA1. The output of LNA1 is fed into the RF input port of MXR1. $IF_1(t)$ and $IF_2(t)$ are multiplied together in MXR1. The IF output of MXR1 is amplified by a video amplifier. The resulting product from MXR1 can be represented by the equation:

$$\text{Video Output} = IF_1(t) IF_2(t) \tag{8}$$

The IF port of MXR1 is not capable of reproducing the high frequency terms resulting from the multiplication of two sinusoidal signals. Therefore the video output of the radar system can be expressed as:

$$\text{Video Output} = \frac{1}{4}\cos[2\pi f_b t] \tag{9}$$

It is clear from the equation above that the video output is the beat frequency difference f_b due to distance from target R and velocity of target v. Thus, we have a homodyne FMCW radar system using two inexpensive microwave transceiver modules.

4. Range Profile Results

The unique approach to FMCW radar has the following specifications:

Center Frequency = 10.25 GHz
Chirp Bandwidth = 70 MHz
Transmit Power = 10 dBm
Front end Noise Figure = 10 dB

Knowing these specifications, several range profiles were taken of standard radar targets placed directly in front of the transmit and receive antennas at some range from the radar system. The range profiles were created by taking the discrete Fourier transform (DFT) of the digitized complex video data. Two range profiles are presented in this paper. Figure 5 is a range profile of a 30 dBsm trihedral corner reflector placed at a range of 25 ft from the radar system. The position of the target is clearly visible in this range profile.

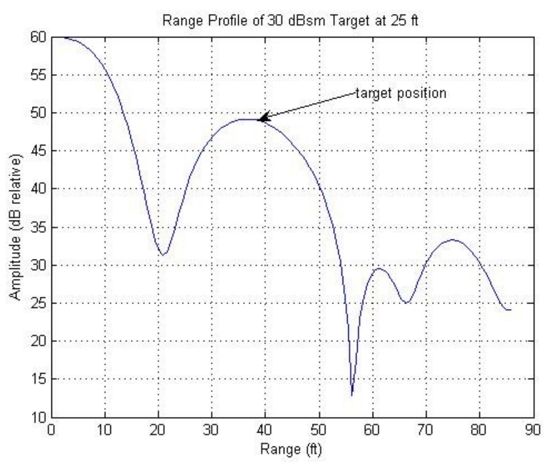

Figure 5: Range profile of 30 dBsm trihedral corner reflector at a range of 25 ft.

Figure 6 is a range profile of a 30 dBsm trihedral corner reflector placed at a range of 40 ft from the radar system. The position of the target is clearly visible in this range profile.

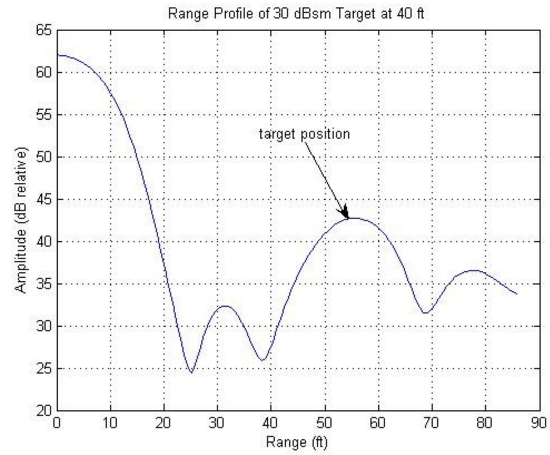

Figure 6: Range profile of 30 dBsm trihedral corner reflector at a range of 40 ft.

Looking at the range profiles shown in figures 5 and 6, it is clear that there is some range offset and non-linear responses occurring. The constant range offset is due to internal hardware cable delays. This will not affect SAR imaging. The slight variation in linear ranging is due to the non-linear tuning of the varactor tuned Gunn oscillator. A tuning linearity plot of the MA87127-1 is shown in [1]. Varactor tuned oscillators in general are not linear. However, this problem must be tolerated in order to operate such an inexpensive radar system.

5. SAR System Implementation

A linear rail SAR was implemented using the unique approach to FMCW radar. A diagram of this implementation is shown in figure 7.

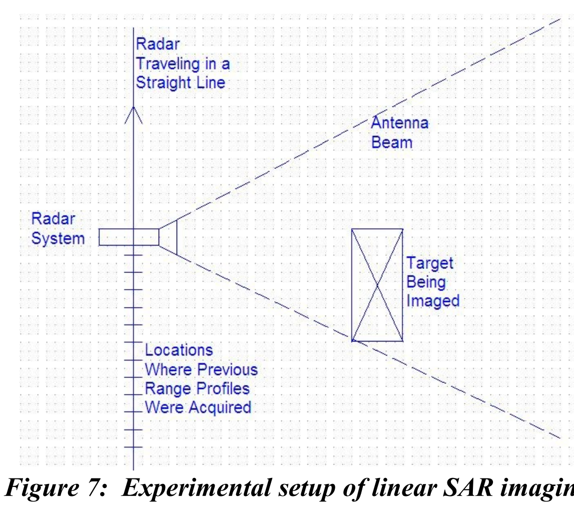

Figure 7: Experimental setup of linear SAR imaging system.

The radar is mounted on a carrier which traverses a 12 foot long linear rail. The transmit and receive antennas are directed away from and perpendicular to the track towards the image scene. Range profiles are acquired at regular intervals as the radar traverses the rail. A picture of this setup is shown in figure 8.

Figure 8: Picture of rail SAR experimental setup. This particular experiment was performed indoors. Shown in the foreground is the linear SAR track, and in the background are two standard radar targets.

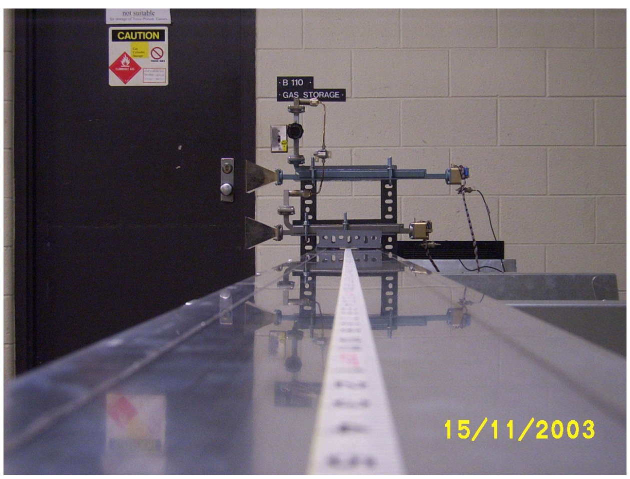

Figure 9: The front end of the unique approach to FMCW radar is moved along the linear SAR rail manually, where the user lines up the front end chassis with measuring tape laid down on the surface of the rail.

Data acquisition is performed using a National Instruments PCI6014 data acquisition card. A Labview VI was programmed to control data acquisitioning and some pre-processing. Data acquisition is triggered by two inputs. The first input results from the VI prompting the user to move the radar manually 1 inch down the track. After the radar is moved 1 inch, the user hits enter. A significant cost savings method used in implementing an ultra low cost SAR imaging system is moving the radar manually and lining up its position with a measuring tape (see figure 9). The VI then waits for an external hardware trigger from a pulse generator. On the rising edge of this trigger, the data acquisition card simultaneously modulates the radar with a linear ramp and digitizes the video output of the radar unit storing the range profile in a 2-D data file. 2000 samples of the video output of the radar unit are digitized at a rate of 200 KSPS. This process is performed every 1 inch until the radar has traversed the entire 12 foot long track. Real over sampled video data is converted to complex I and Q data by use of the formula:

$$S_{complex} = Video\_Output + j * H(Video\_Output) \tag{10}$$

Where: $H(Video\_Output)$ is the Hilbert Transform, and $S_{complex}$ is decimated by 2, throwing out every other sample.

This complex data is compiled into a 2D matrix of radar position vs. range profile. This data is used to create SAR imagery using four different SAR algorithms.

6. Range Stacking Algorithm

A range stacking algorithm was implemented directly from [5]. In this experiment a 20 dBsm trihedral corner reflector was placed 25 ft down range from the rail, and a 30 dBsm trihedral corner reflector was placed 40 ft downrange from the rail. The targets were offset slightly from the center of the rail. The resulting image is shown in figure 10.

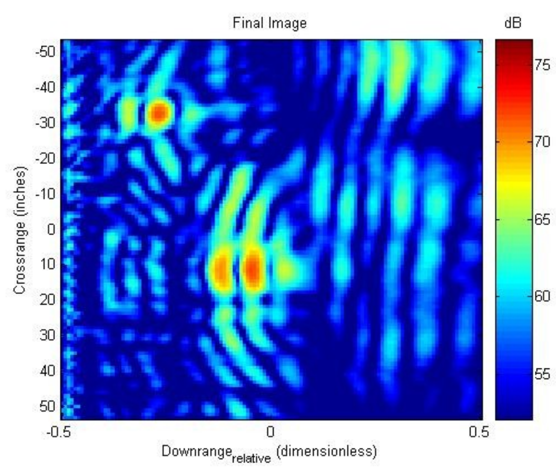

Figure 10: SAR image formed using the range stacking algorithm.

Looking at figure 10, it is clear that the unique approach to FMCW radar in conjunction with a manually operated

SAR rail is capable of producing detailed SAR using a range stacking algorithm. However, it may be possible to create a more focused image using more advanced techniques.

7. The Polar Format Algorithm

Two versions of the PFA were implemented directly from [6]. A target scene was setup with a 20 dBsm trihedral corner reflector located 25 ft from the rail, and a 30 dBsm trihedral corner reflector located 65 ft from the rail. The PFA is based on matched filtering to scene center and non-linear wave number mapping of the radar data. Once these tasks are performed a 2D discrete Fourier transform (DFT) is used to extract the image. Due to wave number mapping of the radar data, an interesting relationship occurs; the shorter the linear SAR rail, the greater the aperture bandwidth. Thus, the shorter the aperture bandwidth, the more curvy the wave number mapping of the radar data becomes. This relationship is explained in [6]. In the case of this particular system, the aperture length is an extremely short 12 ft. The scene center is located at 40 ft from the rail. The transmit bandwidth is only 70 MHz centered at 10.25 GHz. These factors contribute to a curved data mapping which is shown in figure 11.

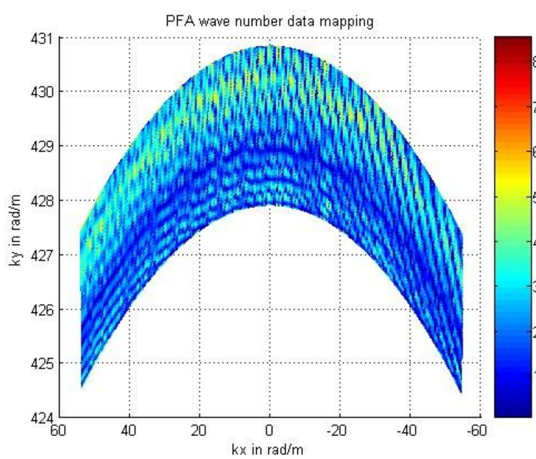

Figure 11: PFA wave number mapping of SAR data, the real part of each data point is shown .

One method of creating PFA SAR imagery from this data is to simply ignore the curvature and assume the data is planar. This is known as the narrow beamwidth and narrow bandwidth assumption. The resulting image using the narrow beamwidth and narrow bandwidth assumption is shown in figure 12.

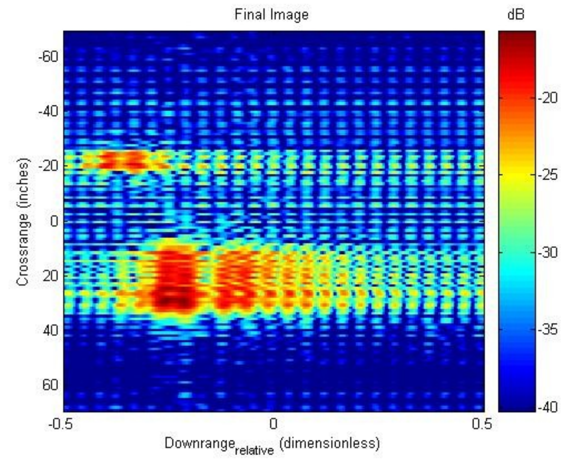

Figure 12: SAR image formed using the PFA with the narrow beamwidth and narrow bandwidth assumption.

It is clear from figure 12 that the image is extremely blurred and unclear. However the PFA with the narrow bandwidth and narrow beamwidth assumption is an extremely fast algorithm, requiring no interpolation. Thus, this algorithm is useful in creating a rough but fast image of a target scene.

A full PFA was implemented. The PFA utilizes a 2D interpolation in the data mapping phase of the algorithm. This takes time, however it forms very detailed imagery. The resulting image using the PFA is shown in figure 13.

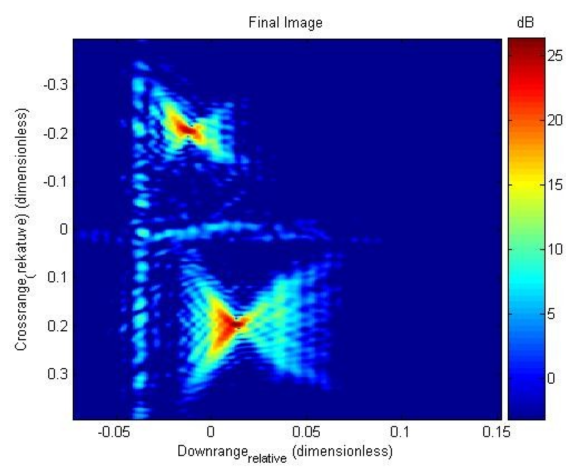

Figure 13: SAR image formed using the PFA.

Looking at figure 13, it is clear that the unique approach to FMCW radar in conjunction with a manually operated SAR rail is capable of producing detailed SAR imagery using the PFA.

8. The Range Migration Algorithm

A RMA algorithm was developed directly from [7]. A target scene was setup with a 20 dBsm trihedral corner reflector located 25 ft from the rail, and a 30 dBsm trihedral corner reflector located 65 ft from the rail. The RMA is similar to the PFA in that wave number data mapping is necessary. However, it differs greatly from the PFA in that the RMA matched filter is a line rather than a point in the scene center. This causes a dramatically different wave number mapping to occur, known as the Stolt interpolation. The Stolt interpolation compensates for geometric distortions in the resulting image due to wavefront curvature. The RMA is faster than the PFA because the Stolt interpolation is only a 1D interpolation. The wave number mapping for the RMA using data collected by the unique approach to FMCW radar is shown in figure 14.

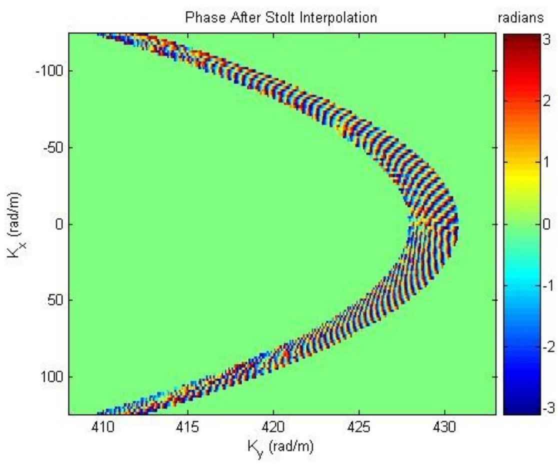

Figure 14: RMA wave number mapping of SAR data, phase of each data point is shown.

After the Stolt interpolation, an inverse 2D DFT process is performed on the data which extracts the image. The resulting image formed using the RMA is shown in figure 15.

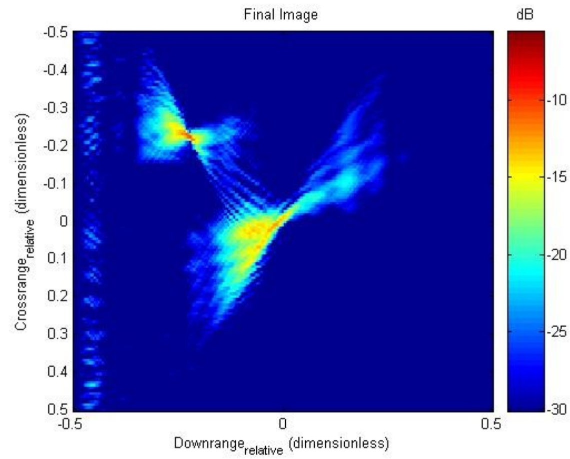

Figure 15: SAR image formed using the RMA.

Looking at figure 15, it is clear that the unique approach to FMCW radar in conjunction with a manually operated SAR rail is capable of producing detailed SAR imagery using the RMA.

6. Conclusions and Future Work

It only takes two 'Gunnplexer' microwave transceiver modules and a few other parts to build a low cost SAR imaging system. From the results presented in this paper, it is clear that SAR imaging on a budget was achieved. The unique approach to FMCW radar was presented and shown to be an inexpensive and fairly precise radar solution. The unique approach to FMCW radar used in conjunction with a manually operated SAR rail was successful at producing SAR imagery using four different imaging algorithms. Two of the four algorithms demonstrated the ability to form detailed imagery using the unique approach to FMCW radar. Future work should include imagery of targets other than trihedral corner reflectors. Future work should also include implementation of this or a similar system at other research institutions or by individuals interested in SAR imaging.

7. References

[1] Charvat, G.L., "A Unique Approach to Frequency-Modulated Continuous-Wave Radar Design." East Lansing MI: A thesis, submitted to Michigan State University, 2003, in partial fulfillment of the requirements for the degree of Master of Science.

[3] Charvat, G.L., Kempel, L. C., "Synthetic Aperture Radar Imaging Using a Unique Approach to Frequency-Modulated Continuous-Wave Radar Design," AMTA Symposium 2005.

[3] Charvat, G.L., Kempel, L. C., “A Unique Approach to Frequency-Modulated Continuous-Wave Radar Design,” AMTA Symposium 2004.

[4] Eaves, J. L., and Ready, E. K. *Principles of Modern Radar.* New York: Van Nostrand Reinhold Company, 1987.

[5] Stimson, G.W., *Introduction to Airborne Radar.* El Segundo, California: Hughes Aircraft Company, 1983.

[6] Soumekh, M., *Synthetic Aperture Radar Signal Processing With MATLAB Algorithms.* New York: John Wiley & Sons, Inc., 1999.

[7] Carrara, W. G., Goodman, R. S., Majewski, R. M. *Spotlight Synthetic Aperture Radar Signal Processing Algorithms.* Boston: Artech House, 1995.